Robust Dynamic Programming Method for Ultrasound Elastography

Ioana Fleming[a], Hassan Rivaz[a], Emad Boctor[b] and Gregory Hager[a]

[a]Johns Hopkins University, [b]Johns Hopkins Medical Institutions, Baltimore, MD, USA

ABSTRACT

Ultrasound elastography is an imaging technology which can detect differences in tissue stiffness based on tissue deformation. For successful clinical use in cancer diagnosis and monitoring the method should be robust to sources of decorrelation between ultrasound images. A regularized Dynamic Programming (DP) approach was used for displacement estimation in compressed tissue. In the Analytic Minimization (AM) extension of DP, integer displacements are calculated just for one RF-line, and later propagated laterally throughout the entire image. This makes the seed RF-line very important; faulty seed lines could propagate erroneous displacement values throughout the image resulting in the appearance of false "lesions". In this paper we analyze the robustness of this method in free-hand palpation of laboratory tissue phantoms. We are proposing an update to the algorithm which includes a random search for the most robust seed RF-line. Axial integer displacements are obtained on each random seed line individually with DP optimization. For each random axial RF-line, multiple random values for decorrelation compensation are used in the displacement estimation. The displacement values are then compared and several metrics of stability and consistency are considered. A ranking is established and the line deemed most robust will become the seed line for displacement propagation, while also selecting the most stable value for decorrelation compensation. The random search can be achieved at no additional computational cost in a parallel implementation. The results indicate significant improvement in the robustness of the DP approach, while maintaining real-time computation of strain images.

1. BACKGROUND AND RATIONALE

Ultrasound Elastography is an imaging technology which can detect differences in tissue stiffness based on tissue deformation.[1] Our work in this paper focuses on real-time quasi-static elastography. The tissue is compressed and relaxed in a continuous free-hand motion and ultrasound images are simultaneously acquired. This method is easy to use and also cheap as it requires no extra hardware. This makes it particularly appealing for medical imaging applications; diagnosis or monitoring could be done at the patient's bed side. There are two hurdles which once resolved would ensure success for clinical use: real-time computation of strain images and dealing with the potential for global and local decorrelation between pre- and post-compression ultrasound signals. Various sources of decorrelation are affecting the computation of strain images in *in-vivo* data, such as incoherent fluid (blood) motion, out-of-plane motion of structures within one image due to transducer or respiratory motion, subsample speckle motion, and a high degree of compression.

Rivaz and Hall initially proposed optimizing a recursive regularized cost function using Dynamic Programming (DP).[2,3] The method resulted in integer values for axial displacement and subsample displacement could also be achieved but at a high computational cost. Rivaz et al. refined the method further using a 1D and 2D Analytic Minimization (AM) of the cost function.[4] It takes the integer displacement of a single axial radio frequency (RF)-line from DP and produces the subsample axial and lateral displacement fields for the entire image.

In this work we analyze the robustness of the AM2D method. Since this method is based on computing integer displacements using DP on only one RF-line, it is crucial that we choose a starting line with little or no decorrelation between the two images. Here we present a method for identifying robust, stable lines and reducing the potential to generate artifact lesions.

Medical Imaging 2012: Ultrasonic Imaging, Tomography, and Therapy, edited by Johan G. Bosch, Marvin M. Doyley, Proc. of SPIE Vol. 8320, 83201K · © 2012 SPIE
CCC code: 1605-7422/12/$18 · doi: 10.1117/12.911879

2. 2D AM SUBPIXEL DISPLACEMENT ESTIMATION

Here we briefly review the 2D AM method in which 2D integer displacements are first obtained using DP on a single RF-line and are then used to produce 2D subsample displacements for the entire image.

1. Calculate integer axial a_i and lateral l_i displacements of one *seed* RF-line using DP ([2]). Calculate an initial subsample estimate using linear interpolation of the integer displacements.

   Let I_1 and I_2 be two ultrasound images acquired before and after deformation. Let m be the number of RF-lines. Each signal is sampled at $i = 1,\ 2 \cdots m$. A regularized cost function is generated combining the prior of displacement continuity (regularization term) and an amplitude similarity term. The displacement continuity term for line j can be written as:

   $$R_j(a_i, l_i, a_{i-1}, l_{i-1}) = \alpha_a (a_i - a_{i-1})^2 + \alpha_l (l_i - l_{i-1})^2 \tag{1}$$

   where α_a and α_l are axial and lateral regularization weights respectively.

   The regularized cost function at the ith sample of the jth A-line becomes:

   $$C_j(a_i, l_i, i) = [I_1(i,j) - I_2(i + a_i, j + l_i)]^2 + \min_{d_a, d_l} \left\{ \frac{C_j(d_a, d_l, i-1) + C_{j-1}(d_a, d_l, i)}{2} + w R_j(a_i, l_i, d_a, d_l) \right\} \tag{2}$$

   where w is a regularization weight for smoothness; d_a and d_l are temporary axial and lateral displacements which are varied in order to minimize eqn. (2).

2. Calculate subsample axial and lateral displacements for the *seed* RF-line using 2D AM (below). They will be added to the initial integer estimates.

3. Propagate the solution of the *seed* RF-line to the left and right. using the displacement of the previous line as initial estimate.

   The aim is to calculate Δa_i and Δl_i such that the duple $(a_i + \Delta a_i, l_i + \Delta l_i)$ gives the axial and lateral displacements at the sample i. The regularized cost function becomes:

   $$\begin{aligned} C_j(\Delta a_1, ..., \Delta a_m, \Delta l_1, ..., \Delta l_m) = \textstyle\sum_m^{i=1} \{ & [I_1(i,j) - I_2(i + a_i + \Delta a_i, j + l_i + \Delta l_i)]^2 + \\ & + \alpha \left(a_i + \Delta a_i - a_{i-1} - \Delta a_{i-1}\right)^2 + \beta_a \left(l_i + \Delta l_i - l_{i-1} - \Delta l_{i-1}\right)^2 + \beta_l^{'} \left(l_i + \Delta l_i - l_{i,j-1}\right)^2 \} \end{aligned} \tag{3}$$

   ,where the index j was dropped for the j^{th} RF-line and $l_{i,j-1}$ is the lateral displacement of the previous RF-line (except for the *seed* line where $l_{i,j-1} = l_i$. α, β_a and $\beta_l^{'}$ are regularization terms which ensure continuity in displacements with respect to the top (axial α), and the top and left/right (lateral β_a and $\beta_l^{'}$). If the displacement of the previous line is not accurate, it will affect the displacement of the next line through the last term in the right-hand side of (3).

3. EXPERIMENTAL DESIGN AND RESULTS

For experimental evaluation we palpated a breast elastography phantom with a 10mm ϕ lesion and three times stiffer than the background. RF data was acquired with a 7.27MHz linear array at a sampling rate of 40MHz. In order to evaluate the magnitude of the problem, we first set out to evaluate the percentage of *seed* RF-lines with faulty DP displacement estimations. When propagated laterally to the neighboring lines, these faulty displacement estimations would result in artifact lesions, clearly visible on the final elastogram (Fig. 1). Many of the artifacts created by the erroneous displacement estimation were very small (Fig. 1 b) and localized at the

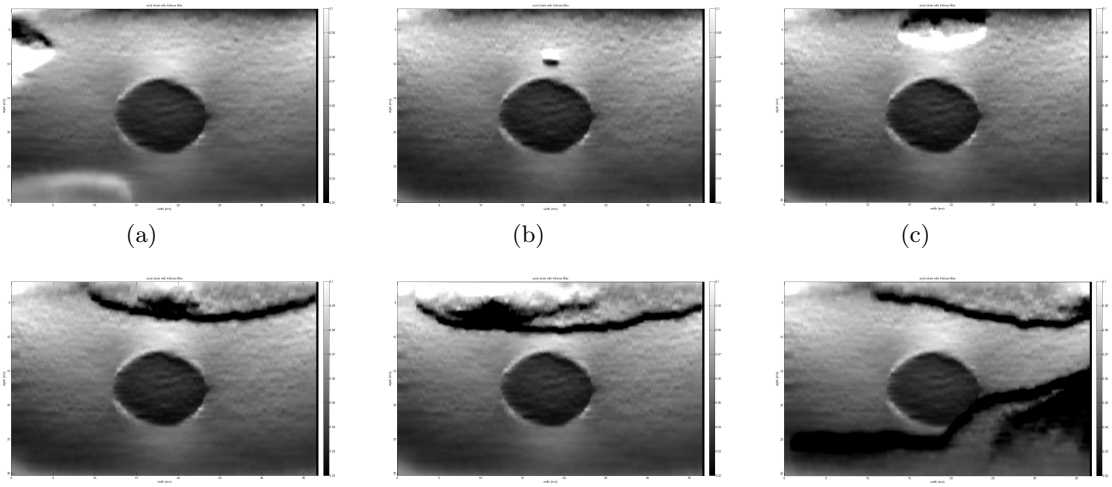

Figure 1. Examples of art1fact lesions in strain images using DP AM2D method. Data collected from breast phantom freehand palpation.

top of the image (Fig. 1 b, c). Some artifacts were however large, sometimes propagating through a big part of the image (Fig. 1 d, e) and, in very rare cases, obscuring the real lesion (Fig. 1 f).

DP displacement computation uses a smoothness regularization parameter w (2), which should prevent regions with high local decorrelation from introducing errors in displacement estimation, but if chosen too large would result in oversmoothing. Strain images were obtained with the AM2D method using each RF-line as a *seed*, each for 11 (eleven) values for w: 0.1, 0.15, 0.2, 0.25, 0.3, 0.35, 0.4, 0.45, 0.5, 0.55 and 0.6. Each resulting elastogram was visually inspected for the presence of artifacts, knowing the shape and size of the expected lesion. The percentages of faulty and good *seed* lines are summarized in Table 1. Some lines produced very faint, very small artifacts on the order of a couple of pixels which were not clearly visible at first inspection and they were categorized as *indeterminate*.

Table 1. Percentage distribution of AM2D behavior for *seed* RF-lines given multiple values for w (smoothness regularization parameter)

w	Good Lines (%)	Faulty Lines (%)	Indeterminate (%)
0.10	44.2	55.8	-
0.15	57.8	42.2	-
0.20	61.3	33.6	5.1
0.25	68.1	30.0	1.9
0.30	65.0	30.5	4.5
0.35	61.7	32.0	5.3
0.40	53.3	41.8	4.9
0.45	53.1	46.9	-
0.50	43.4	56.6	-
0.55	32.1	67.9	-
0.60	24.3	75.8	-

The results were very revealing both about the importance of the value of w, but also of the magnitude of the decorrelated areas. We noted that faulty lines did not appear to be predominant in certain locations, like for example towards the lateral margins of the imaged area, but they were actually widely dispersed throughout the image. In light of the results, for this specific data set we continued our investigation only for w in the range $(0.25, 0.35)$, to ensure a high probability of finding a good starting RF-line.

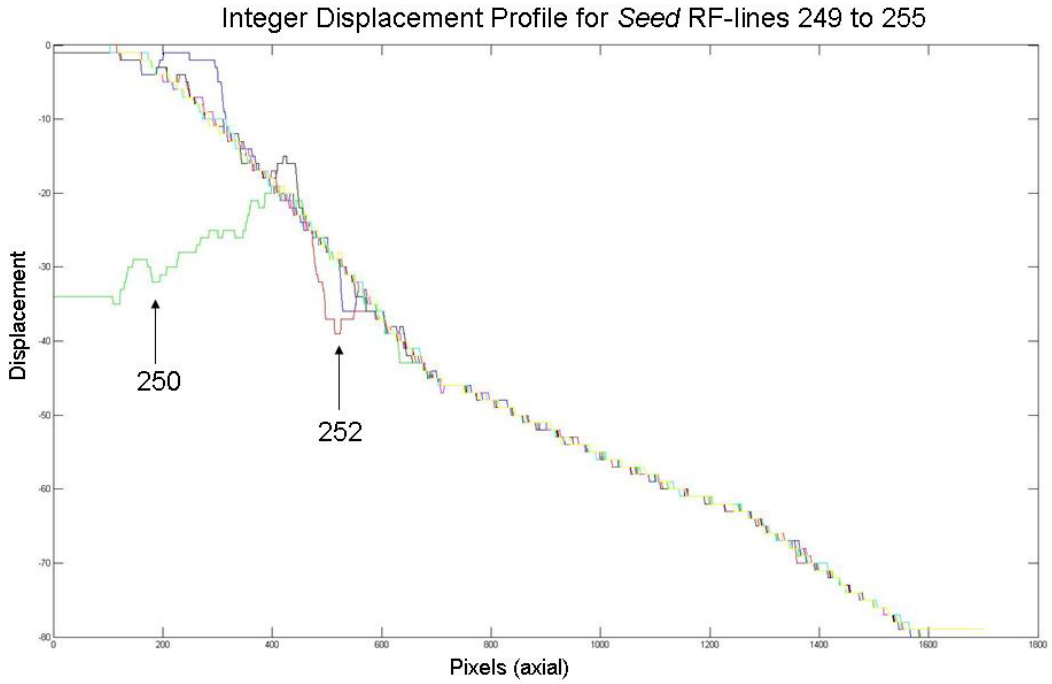

Figure 2. Integer DP displacement estimation for *seed* RF-lines 249 to 255. Note the areas (for lines 250 and 252 respectively) where the change in slope produces the artifact lesions

3.1 *Deformation Slope*

In a continuous piece of tissue, the deformation field resulting from a stress field induced by applied compression has a monotonous ramp profile.[5] Our hypothesis was that faulty lines would exhibit a perturbation in the monotonously decreasing slope of their displacement profile. For example, when plotting DP displacement values for *seed* RF-lines 249 to 255 (Fig. 2), faulty lines 250 and 252 respectively exhibited a change in slope towards the top portion of the imaging area, which in the end resulted in artifact lesions (Fig. 1 c - 250 and b - 252).

A *change-in-slope* parameter was computed for the DP displacement profile for each *seed* RF-line, for w= $0.25, 0.30, 0.35$. 486 lines were evaluated for each of the three values for w, for a total of 1458 computations. The *change-in-slope* test was considered positive when the 3 (three) or more positions exhibited a continuous change in the slope of displacement. Note that the 3 (three) positions did not need to be consecutive, as long as the ramp stayed flat or continued the change direction(Fig. 3 a, b).

3.2 *Displacement Stability*

Another measure of robustness is stability. A robust *seed* RF-line needs to exhibit the same or similar DP displacement estimation across different w values. We computed the percentage of positions (pixels) for which displacement values differed more than 3 (three) pixels between different values of w. For all 486 lines, 3 (three) pairs of displacement values were compared: 1) $w = 0.25$ vs. $w = 0.30$, 2) $w = 0.30$ vs. $w = 0.35$, 3) $w = 0.25$ vs. $w = 0.35$. The score received by each line was averaged over the three comparisons for a final score, potentially ranging from 0 to 1 (100% of pixels exhibited more than 3 (three) pixels differences). We wanted to test the statistical significance of the difference between the faulty lines population and the robust lines population.

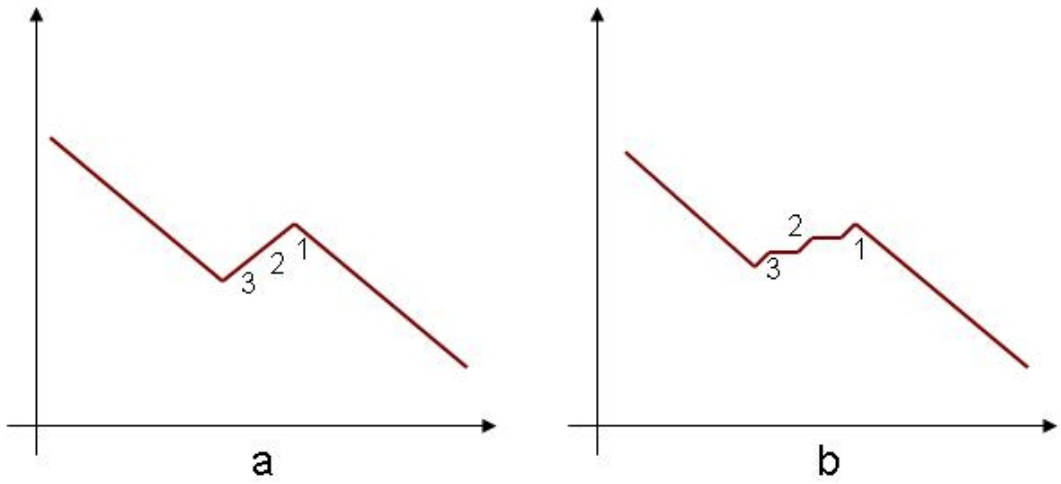

Figure 3. *Change-in-slope* detection algorithm. The 3 (three) positions where the change in slope is exhibited could be consecutive (a) or not (b)

4. RESULTS AND DISCUSSION

4.1 *Deformation Slope*

For a robust AM2D algorithm one single successful *seed* RF-line is sufficient. The *change-in-slope* parameter was designed to select good *seed* lines with monotonously increasing/decreasing displacement profile. Over all 1458 computations of the parameter (486 lines * 3 w values), the sensivity for selecting a good line was **91.7%**, while the specificity was **48.6%** (Table 2). The measure performed up to 93.1% sensitivity when tested across just one w value. We concluded the measure was promising but not sufficient on its own.

Table 2. *Change-in-Slope* (TP = true positive, FP = false positive, TN = true negative, FN = false negative)

		Prediction outcome		
		p	**n**	**total**
actual value	p′	TP = 835	FN = 238	P′
	n′	FP = 76	TN = 252	N′
	total	P	N	

4.2 *Displacement Stability*

486 scores were computed, one for each potential *seed* RF-line. The scores ranged from 0 to 0.2649. The average score for the good lines was 0.0058 (stdev = 0.0186) and the average score for the faulty lines was 0.0444 (stdev = 0.0586). A one-side Student t-test showed a **p-value** of $3.73909e-17$ (Table 3).

To increase the significance of the prediction value, we also computed a combined score for the two detection algorithms. The averaged *Change-in-Slope* score over the 3 (three) values for w was either 0, 0.33, 0.66, or 1, depending on how many of the three instances were deemed positive by the test. This score was added to the *Displacement Stability* score for a combined overall score. This overall score ranged from 0 to 1.1588. The average score for the good lines was 0.0795 (stdev = 0.2422) and the average score for the faulty lines was 0.4939 (stdev = 0.4444), for a **p-value** of $1.75837e-27$ (Table 3).

Table 3. Robustness score: Displacement Stability vs. Combined score for Displacement Stability + Change-in-Slope

	Displ. Stability		Displ. Stability + Change-in-Slope	
	Good Lines	Faulty Lines	Good Lines	Faulty Lines
Min	0	0	0	0
Max	0.1002	0.2649	1	1.1588
Avg	0.0058	0.0444	0.0795	0.4939
StDev	0.0186	0.0586	0.2422	0.4444
p-value	**3.73909E-17**		**1.75837E-27**	

Following the results of this analysis, a random search algorithm was implemented for the selection of a robust, stable *seed* RF-line as follows:

1. DP integer displacement is calculated for 5 random RF-lines, each at 5 random w values
2. A combined *Change-in-Slope* average plus *Displacement Stability* average score is computed
3. The most robust, stable line is chosen as the line with the smallest combined score, which also does not have any positive *Change-in-Slope* score
4. The chosen *seed* line's displacement values are propagated using the AM2D method

Given the current parallel computational resources, the addition of this selection test does not add a significant amount of time to the overall running time. DP takes the same time as before but it's now computed 25 times, and the computation of each score takes on the order of a couple of milliseconds. On 100 random runs of our testing algorithm, we only encountered 1 (one) situation where a faulty line was selected. The reason for the selection was that all 5 of the random line tested were faulty. This prompted us to introduce the additional condition that the chosen line should not have any positive *Change-in-Slope* score. Following this modification, no faulty situation has been encountered so far. We will continue to test our algorithm on the presented data set, as well as on new *ex-vivo* and *in-vivo* tissue data.

5. CONCLUSION

We proposed and successfully implemented an algorithm for the selection of a robust, stable RF-line to be used as *seed* for the DP displacement estimation and later propagated using the AM2D algorithm for elastography. The benefit of this algorithm is significant as it has the potential to improve the robustness of ultrasound elastography in *in-vivo* tissue which can be highly decorrelated. We are in the process of evaluating this hypothesis. The selection of robust *seed* RF-lines becomes even more important as we move towards real-time 3D ultrasound elastography.

REFERENCES

[1] J. Ophir, S. K. Alam, B. Garra, F. Kallel, E. Konofagou, T. Krouskop, T. Varghese, Elastography: ultrasonic estimation and imaging of the elastic properties of tissues, Proceedings of the Institution of Mechanical Engineers. Part H, Journal of Engineering in Medicine 213 (3) (1999) 203–233.

[2] H. Rivaz, E. Boctor, P. Foroughi, R. Zellars, G. Fichtinger, G. Hager, Ultrasound elastography: a dynamic programming approach, IEEE Transactions on Medical Imaging 27 (10) (2008) 1373–1377.

[3] J. Jiang, T. Hall, A regularized real-time motion tracking algorithm using dynamic programming for ultrasonic strain imaging, in: IEEE Ultrasonics Symp., Vancouver, Canada, 2006, pp. 606–609.

[4] H. Rivaz, E. M. Boctor, M. A. Choti, G. D. Hager, Real-time regularized ultrasound elastography, IEEE Transactions on Medical Imaging 30 (4) (2011) 928–945.

[5] G. Mase, Continuum Mechanics for Engineers, Third Edition (Computational Mechanics and Applied Analysis).